J Therm Anal Calorim (2010) 102:579–585
DOI 10.1007/s10973-010-0953-z

Effects of cumene hydroperoxide on phenol and acetone manufacturing by DSC and VSP2

Chun-Chin Huang · Jiou-Jhu Peng · Sheng-Hung Wu · Hung-Yi Hou · Mei-Li You · Chi-Min Shu

NATAS2009 Special Issue

Abstract Cumene hydroperoxide (CHP) being catalyzed by acid is one of the crucial processes for producing phenol and acetone globally. However, it is thermally unstable to the runaway reaction readily. In this study, various concentrations of phenol and acetone were added into CHP for determination of thermal hazards. Differential scanning calorimetry (DSC) tests were used to obtain the parameters of exothermic behaviors under dynamic screening. The parameters included exothermic onset temperature (T_0), heat of decomposition (ΔH_d), and exothermic peak temperature (T_p). Vent sizing package 2 (VSP2) was employed to receive the maximum pressure (P_{max}), the maximum temperature (T_{max}), the self-heating rate (dT/dt), maximum pressure rise rate ($(dP/dt)_{max}$), and adiabatic time to maximum rate ($(TMR)_{ad}$) under the worst case. Finally, a procedure for predicting thermal hazard data was developed. The results revealed that phenol and acetone sharply caused a exothermic reaction of CHP. As a result, phenol and acetone are important indicators that may cause a thermal hazard in the manufacturing process.

Keywords Acetone · Cumene hydroperoxide (CHP) · Differential scanning calorimetry (DSC) · Phenol · Vent sizing package 2 (VSP2)

C.-C. Huang · J.-J. Peng · C.-M. Shu (✉)
Department of Safety, Health, and Environmental Engineering, National Yunlin University of Science and Technology (NYUST), 123, University Rd., Sec. 3, Douliou, Yunlin 64002, Taiwan, ROC
e-mail: shucm@yuntech.edu.tw

S.-H. Wu
Doctoral Program, Graduate School of Engineering Science and Technology, NYUST, Douliou, Yunlin 64002, Taiwan, ROC

H.-Y. Hou
Department of Occupational Safety and Health, Jen-Teh Junior College of Medicine, Nursing and Management, 1, Jen-Teh Rd, Houlong, Miaoli 35664, Taiwan, ROC

M.-L. You
Department of General Education Center, Chienkuo Technology University, 1, Chieh-Shou N. Rd, Changhua 50094, Taiwan, ROC

List of symbols

C_{01}	Initial concentration (mol L^{-1})
C_v	Heat capacity of the sample under constant volume per mass (mol L^{-1})
C_{vR}	Heat capacity of the reactor or vessel under constant volume per mass (mol L^{-1})
dT/dt	Self-heating rate (°C min^{-1})
E_a	Activation energy (kJ mol^{-1})
k_0	Frequency factor (mol L^{-1} s^{-1})
m_0	Mass of the sample (g)
m_R	Mass of the reactor vessel (g)
P_{max}	Maximum pressure (psig)
T_0	Exothermic onset temperature (K)
T_{01}	Initiation temperature of a sample (K)
T_{max}	Maximum temperature (K)
T_p	Exothermic peak temperature (K)
T_s	Self-heating temperature (K)
ΔH_d	Heat of decomposition (kJ kg^{-1})
$(dT/dt)_{max}$	Maximum self-heating rate (°C min^{-1})
$(TMR)_{ad}$	Adiabatic time to maximum rate (min)
$(dP/dt)_{max}$	Maximum pressure rise rate (psig min^{-1})
Φ	Thermal inertia (dimensionless)

Introduction

Phenol is one of the pivotal basic chemicals in the organic chemical industry. It can be used for broad purposes, e.g., manufacturing phenol aldehyde resins, aminocaprolactam, alkyl phenol, preparing pesticides, medicines, and so on [1]. Furthermore, with the rapid increase of synthetic materials, the demand for phenol has increased in Taiwan [2]. Acetone is another key chemical. It can be used for manufacturing methyl methacrylate, bisphenol A and other chemicals, such as ketone, methyl vinyl ketone, isopropyl amino, isophorone, β-irisone, etc. In addition, acetone plays a very critical role in the chemical and other industries as a favorable solvent [3].

The first report of phenol and acetone being produced by acid-catalyzed decomposition of cumene hydroperoxide (CHP) was in 1944 [4]. Hock and Lang use boiling 10% aqueous sulfuric acid to affect the conversion to phenol and acetone. At present, about 94.5% of phenol in the chemical market is manufactured by CHP decomposition [5]. The main mechanism is shown in Fig. 1. However, CHP is a typical organic peroxide (OP) that could result in a fire and explosion owing to the relatively weak oxygen–oxygen linkage (bond dissociation energy of 20–50 kcal mol^{-1}) [6–8]. For the process safety research, the effects of acids, bases, and metal ions on the thermal decomposition of CHP have been investigated [9–11]. This study focused on the phenol and acetone mixed with CHP to recognize the influence of products in the decomposition of CHP and the possible effects in a practical process.

Differential scanning calorimetry (DSC) was utilized to resolve the exothermic behaviors, such as exothermic onset temperature (T_0), exothermic peak temperature (T_p), heat of decomposition (ΔH_d). Vent sizing package 2 (VSP2) was employed to receive the maximum self-heating rate $((dT/dt)_{max})$, maximum pressure rise rate $((dP/dt)_{max})$, adiabatic time to maximum rate (TMR_{ad}), and non-condensable pressure under adiabatic condition in the worst case. Finally, we could obtain the kinetic parameters by Townsend and Tou as well as others [12]. Thermodynamics and kinetic information for the runaway reaction were developed from the adiabatic calorimeter in 1980 [12].

Methods

DSC tests

The preliminary thermal analysis was achieved on a Mettler TA8000 system DSC821^e. The test cell (Mettler ME-26732) was sealed manually by the special tool equipped with Mettler's DSC, which could resist high pressure until about 100 bar. STAR^e software was adopted to determine exothermic curves and to calculate the kinetic parameters. In this study, scanning rate chosen for the temperature-programmed ramp was at 4 °C min^{-1} to possess a better access to thermal equilibrium. For gaining the experimental data, about 4–6 mg of the testing sample was used. The test cell was directing the dynamic scanning by beginning the programmed setting [13].

VSP2 tests

VSP2 is a PC-controlled adiabatic calorimeter manufactured by Fauske and Associates, LLC (FAI). The patented features of the low heat capacity of the cell (112 mL) design along with automatic pressure tracking and adiabatic temperature tracking continually ensure that essentially all the reaction heat released remains within the test sample. These prove it to be a useful tool for measuring temperature and pressure trace in relation to time [14]. It has also been the original DIERS bench scale apparatus for characterizing runaway chemical reactions since 1985. Especially, FAI has highlighted these vent sizing features, stressing the ability to directly scale up the acquired data to process vessels, reactors or containers for the purpose of pressure relief system design [15, 16]. In this study, it was used to receive the runaway reaction data and thermokinetic parameters, such as maximum pressure (P_{max}), maximum temperature (T_{max}), self-heating rate (dT/dt), and (TMR_{ad}). For the sake of safely running the test, CHP 10 mass% was employed in this study.

Mathematic formulation

Temperature variation equation

When the heat absorbed by a vessel could not be negligible, the energy balance equation of the adiabatic reaction system is described as:

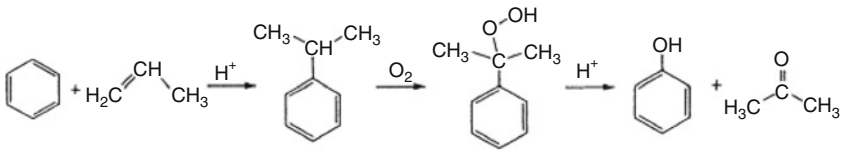

Fig. 1 Main scheme of phenol and acetone process by cumene oxidation [3, 4]

$$\Phi m C_v \frac{dT}{dt} = (-\Delta H) r V \quad (1)$$

where the thermal inertia is defined as:

$$\Phi \equiv \frac{m_s C_v + m_R C_{vR}}{m_s C_v} \quad (2)$$

where m_R mass of the reactor vessel, m_S mass of the sample, C_{vR} heat capacity of the reactor or vessel under constant volume per mass, C_v heat capacity of the sample under constant volume per mass.

The reaction rate equation is expressed as:

$$r = -\frac{dC}{dt}. \quad (3)$$

The above equation is substituted into Eq. 1 and integrated from initial temperature and concentration to final temperature. Here, zero concentration under the assumption of $-\Delta H$, Φ, ρ, and C_v to be constant:

$$\frac{-\Delta H}{\Phi \rho C_v} = \frac{T_f - T_0}{C_0} \quad (4)$$

and

$$\frac{dT}{dt} = \frac{T_f - T_o}{C_o}\left(-\frac{dC}{dt}\right). \quad (5)$$

The adequate concentration–temperature relationship can be obtained by integrating the above equation, and it was approximately:

$$\frac{C}{C_o} = \frac{T_f - T}{T_f - T_o}. \quad (6)$$

For a single nth-order reaction:

$$r = -\frac{dC}{dT} = kC^n \quad (7)$$

with

$$k = k_0 e^{\frac{-E_a}{RT}}. \quad (8)$$

The self-heating rate is obtained from Eqs. 5–8:

$$\frac{dT}{dt} = \left(\frac{T_f - T_o}{C_o}\right) k C_o^n \left(\frac{T_f - T}{T_f - T_o}\right)^n = k\left(\frac{T_f - T}{T_f - T_o}\right)^n (T_f - T_o) C_0^{n-1} \quad (9)$$

so:

$$k = \frac{dT/dt}{C_0^{n-1}\left(\frac{T_f - T}{T_f - T_0}\right)^n (T_f - T_0)}. \quad (10)$$

From Eqs. 9 and 10:

$$\ln k = \ln k_0 - \frac{E_a}{RT} = \ln \frac{dT/dt}{C_0^{n-1}\left(\frac{T_f - T}{T_f - T_0}\right)^n (T_f - T_0)}. \quad (11)$$

Equation 11 could be used to acquire the frequency factor k_0 and the activation energy E_a at the same time [17].

Estimation of initiation temperature

Define the temperature T_0 where the self-heating rate dT/dt equals a small value as the initiation temperature.

The self-heating rate at T_0 is:

$$\left.\frac{dT}{dt}\right|_{T_o} = k\left(\frac{T_f - T}{T_f - T_o}\right)^n (T_f - T_o) C_0^{n-1}\Big|_{T=T_0} = k_0 e^{\frac{-E_a}{RT}} (T_f - T_0) C_0^{n-1}. \quad (12)$$

If the initiation temperature of a sample with an initial concentration C_{01} is T_{01} and that of another sample with C_{02} is T_{02}, then:

$$e^{\frac{-E_a}{RT_{01}}} (T_{f1} - T_{01}) C_{01}^{n-1} = e^{\frac{-E_a}{RT_{02}}} (T_{f2} - T_{02}) C_{02}^{n-1} \quad (13)$$

or

$$\left(\frac{C_{02}}{C_{01}}\right)^{n-1} = e^{\frac{-E_a}{R}\left(\frac{1}{T_{01}} - \frac{1}{T_{02}}\right)} \frac{T_{f1} - T_{01}}{T_{f2} - T_{02}}. \quad (14)$$

From Eq. 14, assuming the heat of reaction, and the density and the heat capacity of the mixture are all constants, then:

$$\frac{T_{f2} - T_{02}}{T_{f1} - T_{01}} = \left(\frac{C_{02}}{C_{01}}\right)\left(\frac{\phi_1}{\phi_2}\right). \quad (15)$$

Substituting Eq. 15 into 14,

$$\left(\frac{C_{02}}{C_{01}}\right)^{n} = e^{\frac{-E_a}{R}\left(\frac{1}{T_{01}} - \frac{1}{T_{02}}\right)} \frac{\phi_2}{\phi_1}. \quad (16)$$

Taking the logarithm on both sides of the Eq. 16:

$$n \ln \frac{C_{02}}{C_{01}} = \frac{-E_a}{R}\left(\frac{1}{T_{01}} - \frac{1}{T_{02}}\right) + \ln \frac{\phi_2}{\phi_1}. \quad (17)$$

Finally, Eq. 18 could be received:

$$T_{02} = \left[\frac{1}{T_{01}} - \frac{R}{E}\left(\ln \frac{\Phi_2}{\Phi_1} - n \ln \frac{C_{02}}{C_{01}}\right)\right]^{-1}. \quad (18)$$

Results and discussion

DSC tests

For a preliminary thermal hazard test, DSC tests were used to observe the difference of exothermic reactions in a specific temperature range, especially for ΔH_d, T_0, and

exothermic peak temperature (T_p). Various ratios of phenol, acetone, mixed with CHP, respectively, could be acquired by using the DSC tests. From DSC thermal curves, Fig. 2 shows the typical heat flow curves versus temperature for the thermal decomposition of 80 mass% CHP in cumene solution with various phenol concentrations. We could recognize that phenol took part in the thermal decomposition of CHP, which would trigger a catalytic reaction to form a higher exothermic peak than CHP alone. However, with the increasing ratio of phenol, the exothermic became lower. For this reason, this study proposed that the effects of phenol were finite. In other words, the effects of phenol only could arise under a specific mixed ratio. If the amount of added phenol was beyond the specific ratio, it would likely contribute to the ΔH_d. Therefore, it was not observed in the real process. In addition, even though phenol was added into CHP, the pathway of thermal decomposition might be the same due to the similar thermal curve and identical T_0.

Figure 3 displays the typical heat flow curves versus temperature for the thermal decomposition of 80 mass% CHP in cumene solution with various acetone concentrations. Instead of a severe exothermic reaction when phenol was mixed with CHP, a mild thermal curve was derived when acetone was mixed with CHP. However, the exothermic peak was occurred earlier than CHP alone. Therefore, the potential hazards would be likely to occur.

Because the exothermic reaction of CHP blended with phenol was more hazardous than CHP alone, we fixed the concentration of phenol and raised the concentration of acetone for the purpose of determining the possible thermal hazards of three components being mixed together. Figure 4 shows the results that is derived from Fig. 2. Even though we fixed the ratio of phenol, the thermal curves also

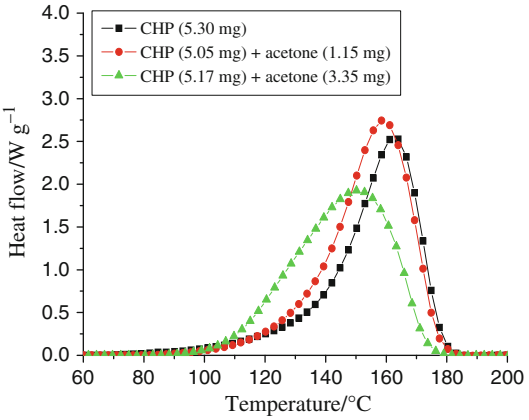

Fig. 3 Thermal curves of various ratios of acetone mixed with CHP by DSC at 4 °C min^{-1}

decreased when the ratio of acetone was increased. This is an entirely different outcome as comparison of Fig. 3. Consequently, the thermal hazards would be confirmed after all series of tests by DSC in this study.

VSP2 tests

From the VSP2 tests, this study could double-check the correspondence of DSC results in this study and discuss the difference between adiabatic condition and kinetic screening. Furthermore, we could realize the thermal hazard if the runaway reaction arose for loss prevention and reducing the frequency of potential disasters. Table 1 lists the detailed setup of this study. Lower ratios of phenol and acetone blended with CHP for the precise results by DSC tests which are revealed in Figs. 5, 6, and 7. Similarly, both the T_p and P_{max} were lessened when the ratio of additive

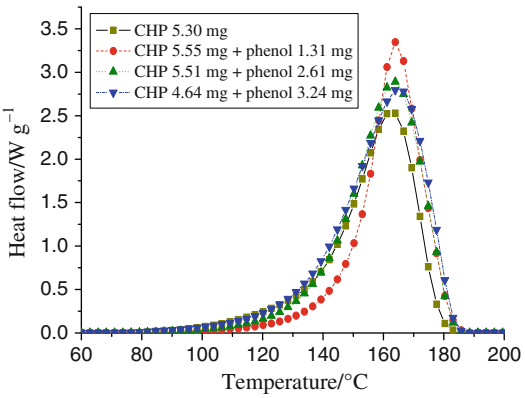

Fig. 2 Thermal curves of various ratios of phenol mixed with CHP by DSC at 4 °C min^{-1}

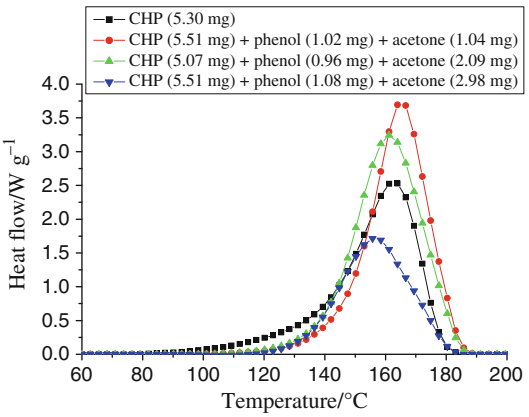

Fig. 4 Thermal curves of various ratios of phenol and acetone mixed with CHP by DSC under 4 °C min^{-1}

Table 1 Experimental setup of VSP2 tests

Component	Series number	Additives (name/mass of additive (g)/percentage in CHP)
CHP	1	–
CHP + phenol	2–1	Phenol/0.25/5%
	2–2	Phenol/0.5/10%
	2–3	Phenol/0.75/15%
CHP + acetone	3–1	Acetone/0.25/5%
	3–2	Acetone/0.5/10%
	3–3	Acetone/0.75/15%
CHP + phenol + acetone	4–1	Phenol/0.25/5%
		Acetone/0.25/5%
	4–2	Phenol/0.25/5%
		Acetone/0.5/10%
	4–3	Phenol/0.25/5%
		Acetone/0.75/15%
	4–4	Phenol/0.25/5%
		Acetone/1.00/20%

Remark: All of CHP samples were in 10 mass% and 50 g

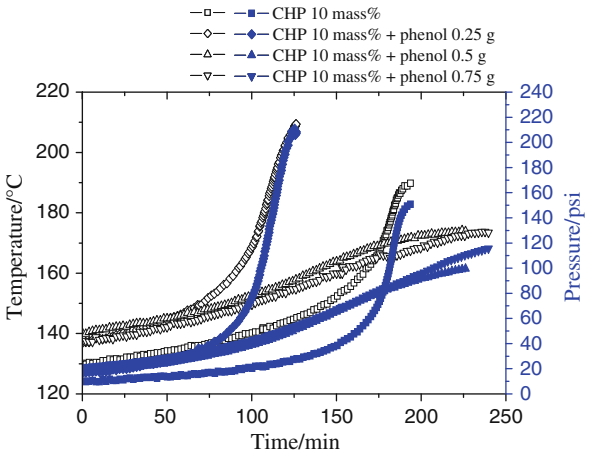

Fig. 5 Temperature (*left*) and pressure (*right*) versus temperature for thermal decomposition of CHP 10 mass% with various amounts of phenol by VSP2 tests

increased in the series tests of phenol mixed with CHP and phenol, acetone mixed with CHP in Figs. 5, 6, and 7. Moreover, the reduction of TMR_{ad} was clearly under adiabatic condition. Especially, acetone caused the TMR_{ad} to be curtailed from 193 to 102 min, as shown in Fig. 6. Therefore, a more severe disaster might be formed by erroneous judgment of emergency response time in a practical process. As a P_{max} result, phenol and acetone would cause a higher T_{max}, P_{max}, and the shorter TMR_{ad} in the thermal decomposition of CHP.

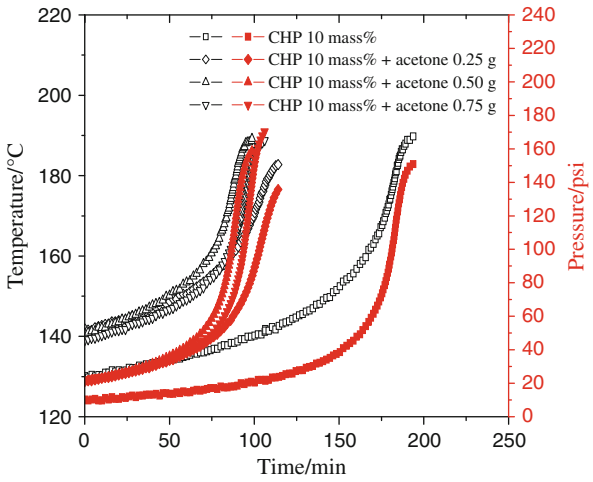

Fig. 6 Temperature (*left*) and pressure (*right*) versus temperature for thermal decomposition of CHP 10 mass% with various amounts of acetone by VSP2 tests

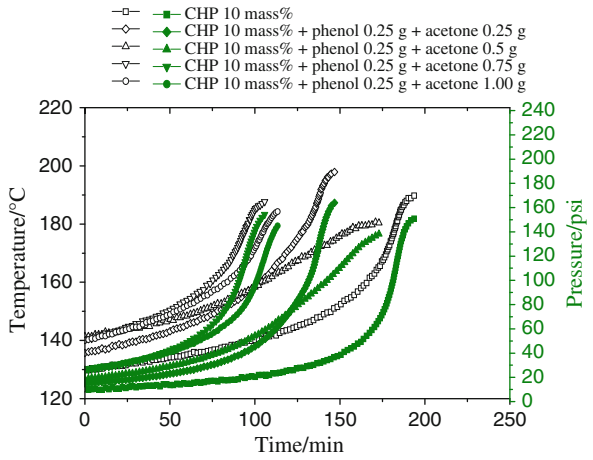

Fig. 7 Temperature (*left*) and pressure (*right*) versus temperature for thermal decomposition of CHP 10 mass% with various amounts of phenol and acetone by VSP2 tests

Thermal hazard prediction by thermokinetic parameters

Based on the worst case of thermal hazard, we deliberately chose the highest T_{max} (CHP 10 mass% + phenol 0.25 g) and the shortest TMR_{ad} (CHP 10 mass% + acetone 0.5 g) from the series of VSP2 tests. The models are mainly described in Eqs. 11 and 18 in this study. It is a valid method to obtain the thermokinetic parameters and to operate the thermal hazard prediction from adiabatic tests. First, we used the linear analysis results by $\ln((dT/dt)/(T_f - T))$ vs. $1/T$ to obtain the E_a and k_0. The calculated results are depicted in Figs. 8, 9, and 10 and the calculated thermokinetic parameters are presented in Table 2 for the purpose of simulating experimental data and thermal hazard prediction.

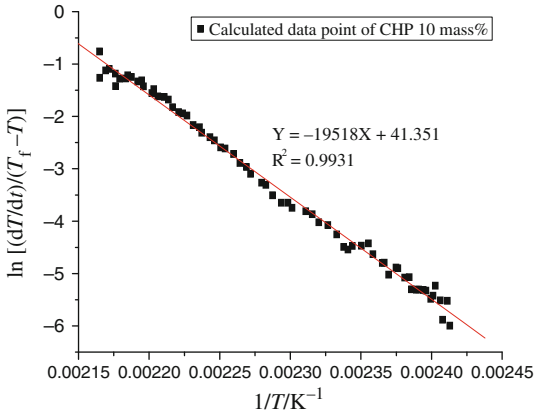

Fig. 8 Estimation of the thermokinetic parameters of CHP 10 mass% from experimental data of VSP2

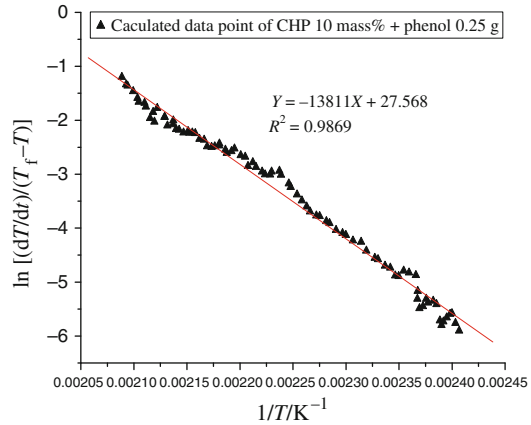

Fig. 9 Estimation of the thermokinetic parameters of phenol mixed with CHP 10 mass% from experimental data of VSP2

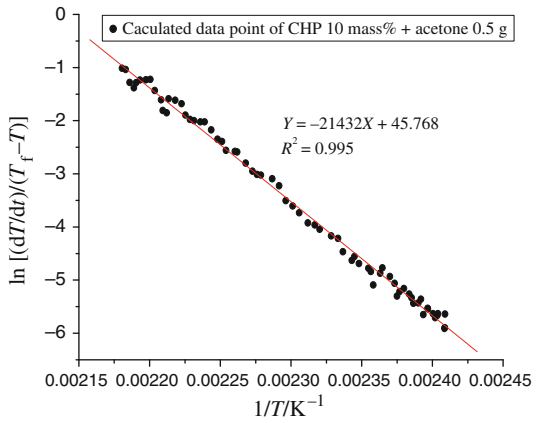

Fig. 10 Estimation of the thermokinetic parameters of acetone mixed with CHP 10 mass% from experimental data of VSP2

Finally, Figs. 11, 12, and 13 compare the temperature variation between the prediction curves for the multiple runaway-reaction models and the experimental data.

Table 2 Calculated thermokinetic parameters from experimental data

Component	E_a/J mol^{-1}	k_0/mol L^{-1} s^{-1}
CHP 10 mass%	161956.7	9.0898×10^{17}
CHP 10 mass% + phenol 0.25 g	115024.2	9.389×10^{11}
CHP 10 mass% + acetone 0.5 g	176980.1	5.545×10^{19}

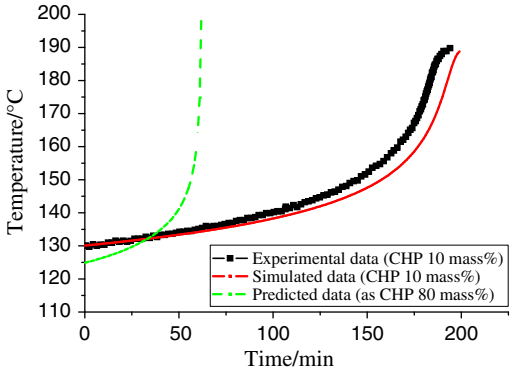

Fig. 11 Time–temperature profiles of experimental data of CHP 10 mass% compared to computer simulation curves and prediction curves

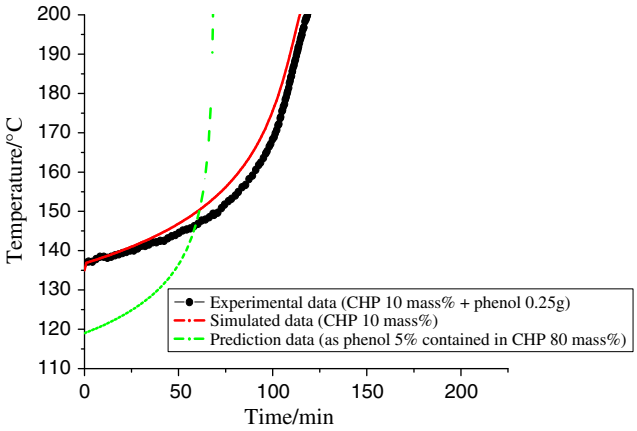

Fig. 12 Time–temperature profiles of experimental data of phenol mixed with CHP 10 mass% compared to computer simulation curves and predicted curves

Therefore, we could surmise that the results of simulations were close to the experimental data. Due to the lower E_a of phenol mixed with CHP, the predicted results showed the mixture was more dangerous than the others in this study. However, even if acetone mixed with CHP caused a shorter TMR_{ad} under adiabatic tests, it would not affect the results of prediction. As far as better accurate prediction is concerned, we might consider the relationship between TMR_{ad} and thermokinetic parameters in the future.

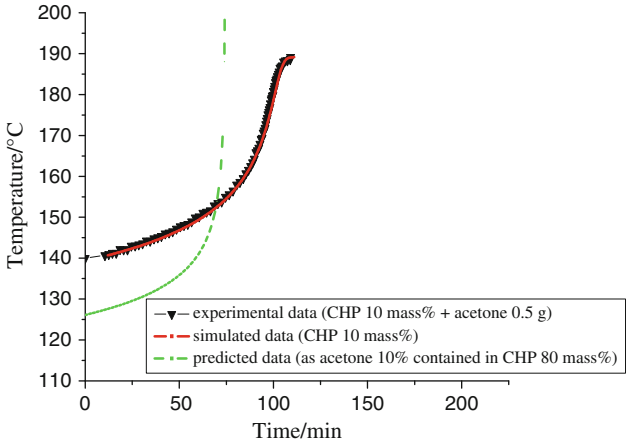

Fig. 13 Time–temperature profiles of experimental data of acetone mixed with CHP 10 mass% compared to computer simulation curves and predicted curves

Conclusions

CHP is a strong reactive OP that easily leads to a runaway reaction. However, it is also the main material for production of phenol and acetone. In this study, the thermal hazards by a series of DSC tests were confirmed when phenol and acetone are mixed with CHP, respectively. In parallel, the course of runaway reaction was performed by VSP2 tests under adiabatic condition for accessing the practical process. From the temperature data, pressure data, and thermokinetic parameters, the potential thermal hazards could be properly narrated that should be paid much attention in terms of loss prevention. In particular, both phenol and acetone would cause the TMR_{ad} of thermal decomposition of CHP to be shorter. It means the emergency response time possibly becomes shorter when acetone and phenol exist in a CHP process rather than CHP alone due to the lower activation energy. In addition, prediction procedures provided the worst case for us to realize the degree of severity. Therefore, the results of this study revealed that the inherently safer design should prudently take into account the incompatible effects of acetone and phenol during CHP production process.

References

1. Kroschwitz JI, Grant MH. Phenol. Encyclopedia of chemical technology, vol 18, 4th edn. USA: Wiley and Sons. p 592.
2. Petrochemical Industry Yearbook. Taiwan, ROC. 2005; 7:2.
3. Huang D, Han M, Wang J, Jin Y. Catalytic decomposition process of cumene hydroperoxide using sulfonic resins as catalyst. Chem Eng J. 2002;88:215–23.
4. Seubold FH, Vaughan WE. Acid-catalyzed decomposition of cumene hydroperoxide. J Am Chem Soc. 1953;75:3790–2.
5. Cao G. Production of phenol/acetone using cumene process. Beijing, PRC: The Chemical Industry Press; 1983. p. 109.
6. Wang YW, Shu CM, Duh YS, Kao CS. Thermal runaway hazards of cumene hydroperoxide with contaminants. Ind Eng Chem Res. 2003;140:1125–32.
7. Levin ME, Gonzales NO, Zimmerman LW, Yang J. Kinetics of acid catalyzed cleavage of cumene hydroperoxide. J Hazard Mater. 2005;130:88–106.
8. Luo KM, Chang JG, Lin SH, Chang CT, Yeh TF, Hu KH, Kao CS. The criterion of critical runaway and stable temperatures in cumene hydroperoxide reaction. J Loss Prev Process Ind. 2001;14:229–39.
9. Suppes GJ, McHugh MA. Solvent and catalytic metal effects on the decomposition of cumene hydroperoxide. Ing Eng Chem Res. 1989;28:1146–59.
10. Chou YP, Huang JY, Tseng JM, Cheng SY, Shu CM. Reaction hazard analysis for the thermal decomposition of cumene hydroperoxide in the presence of sodium hydroxide. J Therm Anal Calorim. 2008;93:275–80.
11. Hou HY, Shu CM, Tsai TL. Reactions of cumene hydroperoxide mixed with sodium hydroxide. J Hazard Mater. 2008;152:1214–9.
12. Townsend DI, Tou JC. Thermal hazard evaluation by an accelerating rate calorimeter. Thermochim Acta. 1980;37:1–30.
13. STARe Software with Solaris Operating System, Operating Instructions, Mettler Toledo, Switzerland; 2004.
14. Fauske & Associates. VSP2 Manual and Methodology, Inc., Burr Ridge, IL, USA; 2002.
15. Leung JC, Fauske HK, Fisher HG. Thermal runaway reactions in a low thermal inertia apparatus. Thermochim Acta. 1986;104:13–29.
16. Leung JC, Greed MJ, Fisher HG. Round-Robin ventsizing package results. Paper presented at the international symphosium on runaway reactions. Cambridge, MA, USA (March);1989. p. 7–9.
17. Liaw HJ, Yur CC, Lin YF. A mathematical model for predicting thermal hazard data. J Loss Prev Process Ind. 2000;13:499–507.